Korean J. Chem. Eng., **31**(11), 2077-2080 (2014)
DOI: 10.1007/s11814-014-0177-1

pISSN: 0256-1115
eISSN: 1975-7220

Exploration for the potential precursors for zirconium carbide atomic layer deposition via comprehensive computational mechanistic study of the gas phase decomposition of neopentyl zirconium derivatives

Yong Sun Won[†]

Department of Chemical Engineering, Pukyong National University, Busan 608-739, Korea

(*Received 20 April 2014 • accepted 24 June 2014*)

Abstract−We previously reported the probable gas phase decomposition mechanism of tetraneopentyl zirconium ($ZrNp_4$) under typical MOCVD (metalorganic chemical vapor deposition) conditions (400 to 800 °C) using computational thermochemistry. By the same approach, we performed a mechanistic study of the gas phase decomposition of trineopentyl zirconium monochloride ($ZrNp_3Cl$) to evaluate its possibility as a CVD precursor for ZrC film growth. It was demonstrated that strong Zr-Cl bonding would require much higher growth temperatures to drive the gas phase decomposition of $ZrNp_3Cl$, compared to $ZrNp_4$. The higher temperature growth would pose the problem of accelerated gas phase parasitic reactions, which potentially hamper ZrC deposition on the surface. However, strong Zr-Cl bonding offers the possibility of ZrC ALD (atomic layer deposition) using dineopentyl zirconium dichloride ($ZrNp_2Cl_2$), and a postulated scheme is presented based on the results from the gas phase decomposition study of $ZrNp_4$ and/or $ZrNp_3Cl$.

Keywords: Trineopentyl Zirconium Monochloride, Dineopentyl Zirconium Dichloride, Tetraneopentyl Zirconium, Zirconium Carbide, Chemical Vapor Deposition, Atomic Layer Deposition, Density Functional Theory

INTRODUCTION

Zirconium carbide (ZrC) has been proposed as a promising cathode material in the application of FEAs (field emitter arrays) [1-6]. It is expected to increase current density without cathode failure (vacuum arc or tip dulling) with the fabrication of cathodes from ZrC, having low work function (4.0 eV) and great hardness (25,467 N/mm_2), or coating of ZrC on conventional cathodes, such as silicon and molybdenum [7-9]. Between the two, the latter (coating of ZrC) is more reasonable due to the lack of a proper etchant for ZrC, unlike silicon, with the conventional FEA fabrication process applied. Moreover, thin layer growth, such as atomic layer deposition (ALD), is necessary for the latter to prevent the decrease of current density due to the curvature increase (tip dulling) [1-6].

We previously reported the synthesis of tetraneopentyl zirconium ($ZrNp_4$) and the successful AA-MOCVD (aerosol-assisted metalorganic chemical vapor deposition) growth of ZrC thin films using $ZrNp_4$ [10,11]. In addition, we demonstrated the probable gas phase decomposition pathways of $ZrNp_4$ via a study of computational thermochemistry [12]. In this study, we present trineopentyl zirconium monochloride ($ZrNp_3Cl$) as an intermediate step in the pursuit of a ZrC ALD precursor. $ZrNp_3Cl$ is commercially available and also possibly prepared according to a procedure given in the literature [13]. Thus, a probable gas phase decomposition pathway of $ZrNp_3Cl$ is investigated through the same computational thermochemistry approach [12], and the possibility of $ZrNp_3Cl$ as a CVD precursor is discussed based on the calculated energetics. Finally, all results from the study of $ZrNp_4$ and $ZrNp_3Cl$ are integrated for the illustration of a probable scheme for ZrC ALD using dineopentyl zirconium dichloride ($ZrNp_2Cl_2$).

COMPUTATIONAL METHOD

All calculations were carried out with the Gaussian 03 program [14], along with the B3LYP DFT method and split basis set (LanL2DZ for zirconium and 6-31G(d) for other elements) [15,16]. Full geometry optimization was performed for all species. The transition state (TS) was optimized using the Berny Algorithm as implemented in the Gaussian 03 program. Harmonic vibration frequencies were calculated for each structure, based on which thermodynamic properties, such as enthalpy and Gibbs energy, were computed for thermochemistry analysis. The GaussView program was utilized for the visualization of the results.

RESULTS AND DISCUSSION

1. Initial Stage of the Decomposition of $ZrNp_3Cl$

We previously demonstrated that decomposition pathways, such as α-hydrogen abstraction and γ-hydrogen abstraction, are much more kinetically favorable than the homolysis of neopentyl in the decomposition of tetraneopentyl zirconium ($ZrNp_4$) [12]. Meanwhile, the cleavage of HCl and CMe_3Cl has to also be considered in the decomposition of $ZrNp_3Cl$. Therefore, the probable initial decomposition pathways of $ZrNp_3Cl$ are summarized as follows:

1) $ZrNp_3Cl \rightarrow \bullet C_5H_{11} + \bullet ZrNp_2Cl$
: neopentyl homolysis

2) $ZrNp_3Cl \rightarrow \bullet C_4H_9 + \bullet CH_2ZrNp_2Cl$
: isobutyl homolysis

3) $ZrNp_3Cl \rightarrow C_{10}H_{12}ClZr + CMe_4$

[†] To whom correspondence should be addressed.

E-mail: yswon@pknu.ac.kr

: α- or γ-hydrogen abstraction of CMe_4

4) $ZrNp_3Cl \rightarrow C_{15}H_{32}Zr + HCl$

: α- or γ-hydrogen abstraction of HCl

5) $ZrNp_3Cl \rightarrow C_{11}H_{24}Zr + CMe_3Cl$

: reductive elimination of CMe_3Cl

For reactions 1 and 2, reaction enthalpy (ΔH^{o}_{298}) values were calculated as 56.2 kcal/mol and 64.9 kcal/mol, respectively. Considering that the reaction enthalpy of the same neopentyl homolysis from $ZrNp_4$ was 57.1 kcal [12], it is likely that the energetics of a reaction involving a certain ligand are rarely affected by the presence of other uninvolved ligands. Thus, the neopentane (CMe_4) cleavage in reaction 3 can be explained by the energetics and pathways obtained in the previous study of the decomposition of $ZrNp_4$. It was concluded that γ-hydrogen abstraction ($\Delta H^{o\ddagger}_{298}$=37.4 kcal/mol) is favorable over α-hydrogen abstraction ($\Delta H^{o\ddagger}_{298}$=40.6 kcal/mol); however, they are competing instead of the dominant preference of γ-hydrogen abstraction from the kinetic aspect [12]. For the HCl cleavage in reaction 4, there are also two possible pathways, as in reaction 3: α- and γ-hydrogen abstractions. Fig. 1 shows the energetics of those two pathways, compared to reactions 1 to 3.

It is demonstrated that the CMe_4 cleavage (reaction 3) is apparently preferred in the initial decomposition of $ZrNp_3Cl$. However, the energetics of other pathways are worth being reviewed because the post-reaction to the first CMe_4 cleavage is supposed to be one of those. The activation energy ($\Delta H^{o\ddagger}_{298}$) of γ-hydrogen abstraction of HCl from $ZrNp_3Cl$ is almost the same as its reaction enthalpy (ΔH^{o}_{298}), as shown in Fig. 1. In addition, both of them are considerably lower than the reaction enthalpy ($\Delta H^{o\ddagger}_{298}$) of α-hydrogen abstraction by the amount of ~27 kcal/mol. This suggests that the HCl cleavage from $ZrNp_3Cl$ (reaction 4) is done by γ-hydrogen abstraction with the dominant preference. Note that alkyl homolyses (reaction 1 and 2) have similar reaction enthalpies to the γ-hydrogen abstraction of HCl (reaction 4). A further reaction, such as dineopentyl (Np_2) formation, will be discussed afterwards.

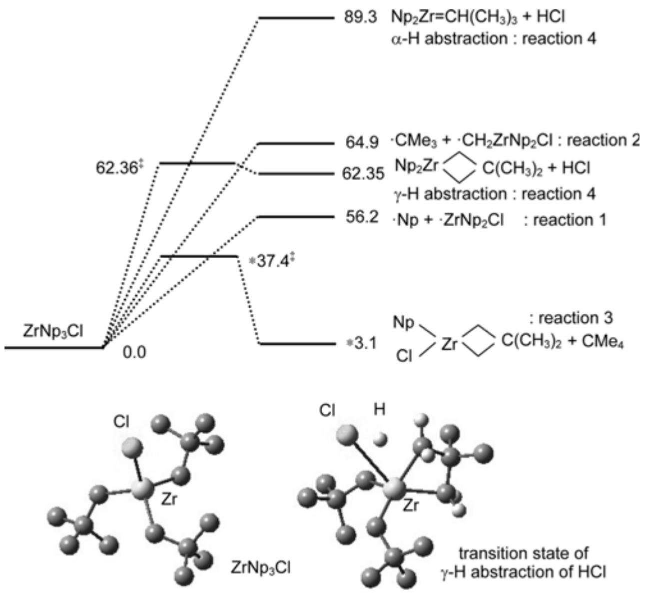

Fig. 1. Energetics of the reactions, 1 to 4, and computed structures of $ZrNp_3Cl$ and transition state of γ-hydrogen abstraction of HCl. All values in energetics are in the unit of kcal/mol. The values with the symbol of * include the results obtained in the previous study for $ZrNp_4$ decomposition [12].

For the reductive elimination of CMe_3Cl from $ZrNp_3Cl$ (reaction 5), a much higher energy (~85 kcal/mol) will be required, as shown in Fig. 2. In fact, the location of the corresponding transition state failed; however, the activation energy of this step is probably not much larger than its reaction enthalpy, similar to the γ-hydrogen abstraction of HCl (see Fig. 1). As an alternative scheme for CMe_3Cl formation, radical (isobutyl and chlorine) homolyses and the subsequent recombination of radicals were considered, and their energetics are also shown in Fig. 2. Clearly, CMe_3Cl formation through

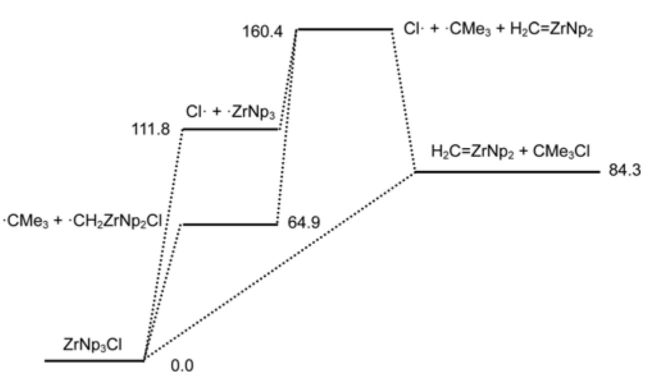

Fig. 2. Energetics of reaction 5, recombination of isobutyl, and chlorine radicals. All values in energetics are in the unit of kcal/mol.

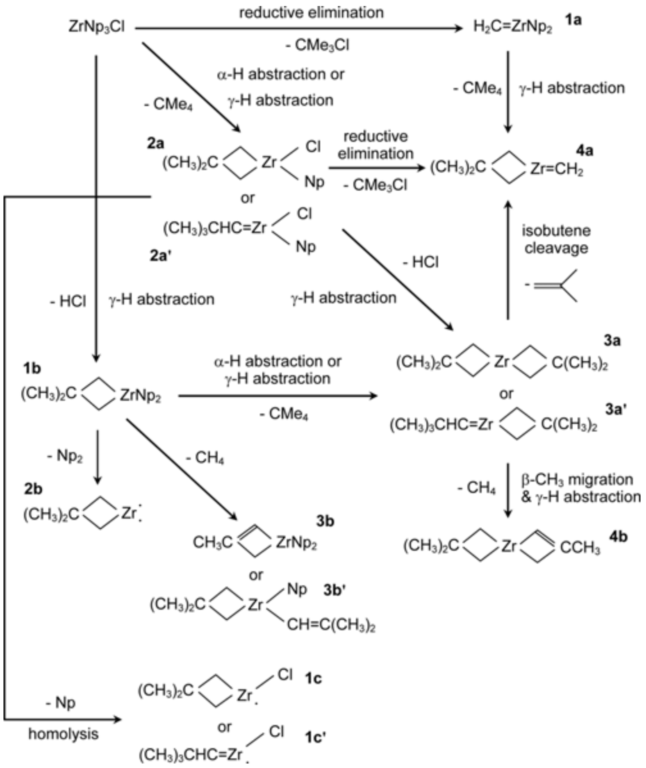

Fig. 3. Decomposition pathways of $ZrNp_3Cl$ in the gas phase under the conventional MOCVD condition (400 to 800 °C) based on computational results.

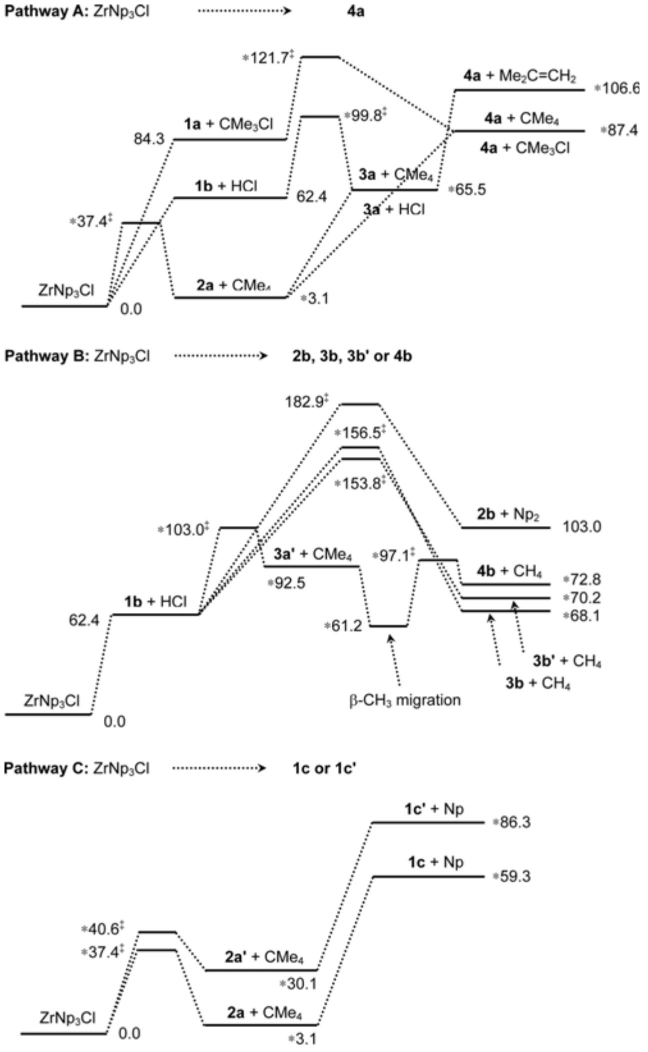

Fig. 4. Energetics of the overall decomposition of ZrNp$_3$Cl, divided into three pathways for simplicity. All values in energetics are in the unit of kcal/mol. The symbol, ‡, denotes transition states. The values with the symbol of * include the results obtained in Fig. 1 and/or in the previous study for ZrNp$_4$ decomposition [12].

radical recombination is not energetically preferred.

2. Overall Decomposition of ZrNp$_3$Cl

Based on the idea discussed above and the previous study of ZrNp$_4$ decomposition [12], we propose the overall decomposition mechanism of ZrNp$_3$Cl, as shown in Fig. 3. It is divided into three different pathways for simplicity, and their energetics are illustrated separately in Fig. 4. As previously mentioned, it is assumed that the activation and reaction energies for some steps are not much different from the corresponding values obtained in Fig. 1 and the previous study of ZrNp$_4$ decomposition [12], as long as participating ligands are the same. For example, the activation and reaction energies of CMe$_4$ cleavage from ZrNp$_3$Cl via γ-hydrogen abstraction must be close to those of CMe$_4$ cleavage from ZrNp$_4$ via γ-hydrogen abstraction, regardless of the kinds of uninvolved ligands. This assumption is only limited to the semi-quantitative comparison to be performed in this study.

We demonstrated in the previous study that the activation energies for the main mechanism steps in the ZrNp$_4$ decomposition are all in a narrow range: 37 to 42 kcal/mol [12]. On the contrary, much higher energies, ranging from 40 to 120 kcal/mol are required to generate main intermediates of ZrNp$_3$Cl, as shown in Fig. 4. In pathway A (see Fig. 4), the pathway to reach **4a** via the reductive elimination of CMe$_3$Cl and the subsequent γ-hydrogen abstraction of CMe$_4$ has a very high activation barrier (121.7 kcal/mol). The pathway possibly stops at the first reductive elimination of CMe$_4$Cl. Instead, it seems that the γ-hydrogen abstraction of CMe$_4$ and the subsequent reductive elimination of CMe$_3$Cl are energetically favorable and finally reach **4a**. The other pathway to get **4a**, the γ-hydrogen abstraction of HCl and the subsequent CMe$_4$/isobutene cleavages, is also less favorable. Pathway B (see Fig. 4) shows possible decomposition pathways starting with the γ-hydrogen abstraction of HCl. The pathway to reach **4b**, including the β-methyl migration and the subsequent γ-hydrogen abstraction of CH$_4$ [12], is the most energetically favorable among them. The formation of dineopentyl ($\Delta H^{o}_{298}=-79.9$ kcal/mol), $Np+Np\rightarrow Np_2$, showed how favorable alkyl radicals could participate in gas phase parasitic reactions by dimerization during MOCVD growth. The energy for the neopentyl homolysis from **1b** was 60.3 kcal/mol (average of the two), and it was not much different from the value for the neopentyl homolysis from ZrNp$_3$Cl, 56.2 kcal in Fig. 1. Pathway C (see Fig. 4) shows a rather simple, but energetically most probable, decomposition pathway. It leads to another chlorine-containing intermediate radical (**1c** or **1c′**). Afterwards, this radical is probably involved in a subsequent step, such as dimerization.

3. The Possibility of ZrNp$_3$Cl as a Precursor for ZrC MOCVD

We reported the successful AA-MOCVD growth of ZrC thin films in the temperature range of 400 to 600 °C [10,11]. However, any deposition was hardly observed at higher temperatures (>700 °C), and it was described with the accelerated gas phase parasitic reactions [10,11]. As shown in Fig. 1, the calculated activation energy for the homolysis of isobutyl or neopentyl was in the range of 55 to 65 kcal/mol, possibly accessible in the higher temperature range of the conventional MOCVD. Therefore, gas phase parasitic reactions are probably kindled by the homolysis of those alkyls. As demonstrated in the previous section, most of the pathways, especially those involving a chlorine cleavage in the overall decomposition of ZrNp$_3$Cl, have quite high energy barriers (>60 kcal/mol). This means that gas phase parasitic reactions will be inevitably overlapped with the main decomposition reactions of ZrNp$_3$Cl. As an example, the pathway to reach **4a**, the intermediate having the most favorable geometry for adsorption on the surface [12], is also energetically less favorable (>85 kcal/mol) than the alkyl homolysis. Pathway C (see Fig. 4) will be another source of gas phase parasitic reactions. As a conclusion, ZrNp$_3$Cl is not promising for ZrC MOCVD film growth because its strong Zr-Cl bonding hampers the gas phase decomposition of ZrNp$_3$Cl to a proper extent.

However, this strong Zr-Cl bonding poses the possibility of dineopentyl zirconium dichloride (ZrNp$_2$Cl$_2$) as an ALD precursor. The proposed scheme for ZrC ALD growth from ZrNp$_2$Cl$_2$ is illustrated in Fig. 5. The activation energies of CMe$_4$ cleavage (b→c) and the subsequent isobutene cleavage (c→d) in the gas phase were about 40 kcal/mol in the previous study of ZrNp$_4$ decomposition [12]. They are possibly accessible, especially if they occur on the surface, even at low operating temperature (<300 °C) of ALD. In the step of a→b,

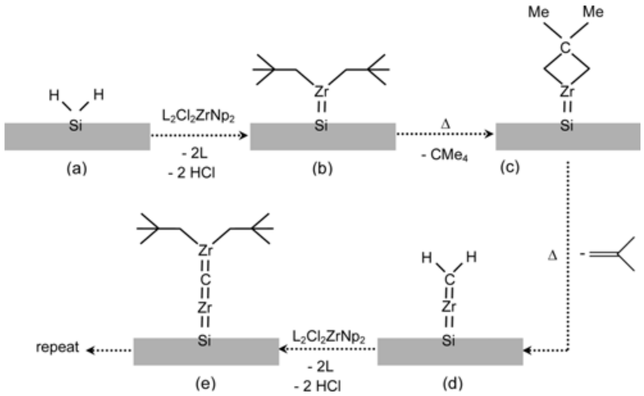

Fig. 5. Proposed scheme for ZrC ALD growth from $ZrNp_2Cl_2$.

the additional ligand, L, is added to secure the chemical stability of the $ZrNp_2Cl_2$ precursor, and it comes off readily at the initial stage. The EtO_2, DME (dimethylether), and TMEDA (tetramethyethylene diamine) can be utilized for this purpose.

CONCLUSION

The probable gas phase decomposition mechanism of trineopentyl zirconium monochloride ($ZrNp_3Cl$) under typical MOCVD conditions (400 to 800 °C) was investigated using computational thermochemistry. Unlike the decomposition of $ZrNp_4$, the calculated energetics for the overall decomposition of $ZrNp_3Cl$ demonstrated that most of the pathways have quite higher energy barriers (>60 kcal/mol), overlapped with, or higher than, the energy barrier of alkyl homolysis. Therefore, the strong Zr-Cl bonding would hamper the proper gas phase decomposition of $ZrNp_3Cl$ even at high temperatures during ZrC MOCVD growth, and gas phase parasitic reactions would dominate. However, the strong Zr-Cl bonding poses a great possibility of dineopentyl zirconium dichloride ($ZrNp_2Cl_2$) as a ZrC ALD precursor, and a postulated scheme was proposed.

ACKNOWLEDGEMENTS

This work was supported by a Research Grant of Pukyong National University (C-D-2014-0314). Most of the calculation work was conducted in the author's graduate study and, thus, the author sincerely thanks the Department of Chemistry at the University of Florida for granting access to the Gaussian program.

REFERENCES

1. W. A. Mackie, R. L. Hartman, M. A. Anderson and R. R. Davis, *J. Vac. Sci. Technol. B*, **12**(2), 722 (1994).
2. W. A. Mackie, T. Xie, M. R. Matthews, B. P. Routh Jr. and P. R. Davis, *J. Vac. Sci. Technol. B*, **16**(4), 2057 (1998).
3. W. A. Mackie, T. Xie and P. R. Davis, *J. Vac. Sci. Technol. B*, **17**(2), 613 (1999).
4. D. H. Kang, V. V. Zhirnov, G. J. Wojak, R. C. Sanwald, M. Park, J. J. Hren and J. J. Cuomo, *Mat. Res. Soc. Symp. Proc.*, **558**, 563 (2000).
5. C. Spindt, C. E. Holland and P. R. Schwoebel, *SPIE Proc.*, **3955**, 151 (2000).
6. J. E. Yater, A. Shih and D. S. Katzer, *Mat. Res. Soc. Symp. Proc.*, **558**, 551 (2000).
7. R. Kieffer, *Proc. Intern. Symp. Reactive Solids*, 1001 (1952).
8. Technical Publications, CERAO incorporate, **7**(2) (1997).
9. T. Aizawa, *Rep. of National Institute for Research in Inorganic Materials*, **81**, 27 (1994).
10. Y. S. Won, Y. S. Kim, O. Kryliouk, T. J. Anderson, V. G. Varanasi, C. T. Sirimanne and L. McElwee-White, *J. Cryst. Growth*, **304**, 324 (2007).
11. Y. S. Won, V. G. Varanasi, O. Kryliouk, T. J. Anderson, L. McElwee-White and R. J. Perez, *J. Cryst. Growth*, **307**, 302 (2007).
12. Y. S. Won, *Korean J. Chem. Eng.*, **29**(10), 1438 (2012).
13. A. K. Hughes and A. J. Kingsley, *Organomet. Chem.*, **539**(1-2), 109 (1997).
14. Gaussian 03, Revision B.04, M. J. Frisch, G. W. Trucks, H. B. Schlegel, G. E. Scuseria, M. A. Rob, J. R. Cheeseman, J. A. Montgomery Jr., T. Vreven, K. N. Kudin, J. C. Burant, J. M. Millam, S. S. Iyengar, J. Tomasi, V. Barone, B. Mennucci, M. Cossi, G. Scalmani, N. Rega, G. A. Petersson, H. Nakatsuji, M. Hada, M. Ehara, K. Toyota, R. Fukuda, J. Hasegawa, M. Ishida, T. Nakajima, Y. Honda, O. Kitao, H. Nakai, M. Klene, X. Li, J. E. Knox, H. P. Hratchian, J. B. Cross, V. Bakken, C. Adamo, J. Jaramillo, R. Gomperts, R. E. Stratmann, O. Yazyev, A. J. Austin, R. Cammi, C. Pomelli, J. W. Ochterski, P. Y. Ayala, K. Morokuma, G. A. Voth, P. Salvador, J. J. Dannenberg, V. G. Zakrzewski, S. Dapprich, A. D. Daniels, M. C. Strain, O. Farkas, D. K. Malick, A. D. Rabuck, K. Raghavachari, J. B. Foresman, J. V. Ortiz, Q. Cui, A. G. Baboul, S. Clifford, J. Cioslowski, B. B. Stefanov, G. Liu, A. Liashenko, P. Piskorz, I. Komaromi, R. L. Martin, D. J. Fox, T. Keith, M. A. Al-Laham, C. Y. Peng, A. Nanayakkara, M. Challacombe, P. M. W. Gill, B. Johnson, W. Chen, M. W. Wong, C. Gonzalez and J. A. Pople, Gaussian, Inc., Wallingford CT (2004).
15. A. D. Becke, *J. Chem. Phys.*, **98**, 1372 (1993).
16. P. J. Stephens, F. J. Devlin, C. F. Chabalowski and M. J. Frisch, *J. Phys. Chem.*, **98**, 11623 (1994).